Solar Energy
And Sustainable Development
Refereed, biannual scientific journal issued by
Center for Solar Energy Research and Studies

Simulation Of Indirect Solar Crop Dryers Augmented With Pebble-Bed Thermal Storages

E.M. Elbenghazi[1], K. R. Agha[2], and E. I. Dekam[2]

[1]M.Sc. Senior Engineer, The General Electrical Company, Libya; [2] Professor in Mechanical and Industrial Engineering Department, Faculty of Engineering, University of Tripoli, Tripoli, Libya.

e-*mail: [1]motasem882002772@hotmail.com; [2]k-r-agha@yahoo.com; [3]eidakkam@hotmail.com*

Abstract: This paper presents a model of indirect solar dryer augmented with pebble bed thermal storage. The thermal storage system was considered to be placed inside the drying chamber above the 47°-tilted air solar collector and below the crop bed, where an average September-daily insolation profile was given for the 32°N location. A presented mathematical model took into consideration the pressure and natural buoyancy forces, employed the basic governing equations, atmospheric-air psychometric-chart relations, and published correlation relationships. A "QBASIC" computer program was written based on the trial and error method for calculation of different parameters. Dimensions of the dryer system, position and characteristics of the crop and storage beds, strongly affected the behavior of the dryer system, for both rice and tomato products. Referring to the considered indirect solar dryer design type, on the average two and five days were required for rice and tomatoes long-term drying, respectively. This seems to be visible in rice products, however, it is far from applicability for tomatoes mass-drying process in agricultural fields, due to its high initial moisture content.

محاكاة مجففات المحاصيل الشمسية غير المباشرة المزودة بخزانات فرش الحصى الحرارية

المعتصم البنغازي[1]، خيري آغا[2]، و الهادي الدكام[2]

[1] الشركة العامة للكهرباء. طرابلس - ليبيا

[2] قسم الهندسة الميكانيكية والصناعية، كلية الهندسة - جامعة طرابلس. طرابلس - ليبيا

ملخص: هذه الورقة تقدم نموذجًا للمجفف الشمسي غير المباشر المزود بفرش من الحصى كخزان حراري. أخذ نظام التخزين الحراري على أنه موضوع داخل غرفة التجفيف فوق مجمع شمسي هوائي يميل 47° وتحت فرش المحصول، حيث يتعرض لمنحى تشميس يومي متوسط في شهر سبتمبر بموقع 32 درجة شمالاً. النموذج الرياضي المقدم يأخذ في الاعتبار قوى الضغط والطفو الطبيعي، وذلك بتوظيف المعادلات الحاكمة الأساسية وعلاقات المخطط السيكرومتري للهواء الجوي والعلاقات الترابطية المنشورة. كتب برنامج حاسوبي «QBASIC» استناداً إلى أسلوب التجربة والخطأ لحساب مختلف المعاملات. جاءت أبعاد منظومة المجفف ومكان وخصائص

فرشتي المحصول والتخزين لتؤثر بشدة في سلوك منظومة المجفف، لكل من منتجات الأرز والطماطم. بالإشارة إلى نوع تصميم المجفف الشمسي غير المباشر المعتمد لهذه الدراسة، كان المطلوب في المتوسط يومين وخمسة أيام للأرز والطماطم للتجفيف طويل الأمد، على التوالي. يبدو أن هذا مجدي لمحصول الأرز، ولكنه بعيد عن التطبيق لعمليات تجفيف الطماطم على نطاق واسع في الحقول الزراعية، نظرًا للمحتوى المائي الابتدائي العالي للطماطم.

Keywords: *Air collector applications, Indirect solar dryers, Rice and tomatoes preservation, Natural hot air flow, Natural buoyancy forces.*

1. INTRODUCTION

One particularly important application of solar energy is in the area of drying of agricultural crops [1]. In dryers, the induced hot air flow may occur naturally due to the buoyancy effect, or forced motion due to fan-related generated differential pressure. There are several geometries-based designs for the indirect solar dryers [2-5].

Many researchers were involved in studying dryers with packed storage bed [6]. Balakrishnan and Pei [2] determined a correlation for the convective heat transfer coefficient between a fluid and the particles of the bed. They used microwave power to heat the bed which resulted in a uniform temperature throughout the bed. Thus, they eliminated thermal gradients within the bed, so that the conduction heat transfer between the particles could be neglected. Gross et al. [7] numerically predicted the temperature distribution in a deep packed bed. They assumed a one-dimensional flow throughout the bed and took into account variations of the properties of the air with temperature.

Oosthuizen [8] suggested that the performance of natural convective solar dryers might be improved if they incorporated energy storage. He presented a layout for the indirect solar dryer indicating the possible locations for the storage media within the system. In an experimental study, the moisture removing rate was reported to increase with the increase in mass of ginger samples and decreases significantly with the progression of drying days [9]. The present study considered the natural or passive-convective indirect-solar dryers, where the induced buoyancy forces resulted from the temperature gradient along the passage of the dryer. The performance of such indirect solar dryers should be improved by employing an energy storage system associated with the solar dryer.

2. THE CONSIDERED TYPE OF SOLAR DRYERS

In this work, a pebble bed thermal energy storage was integrated with the solar-based dryer. A dryer of this type is shown in Figure 1. This solar drying system was prepared before any drying process took place. The preparation stage included accumulating thermal energy in the installed energy storage inside the solar dryer. Once the equilibrium state was reached, the crop was placed in the specified trays, and drying process was started. The process uses the incoming solar energy in the solar collector beside the stored thermal energy in the pebble bed storage. This combination is desired to enhance the process by achieving acceptable drying rates.

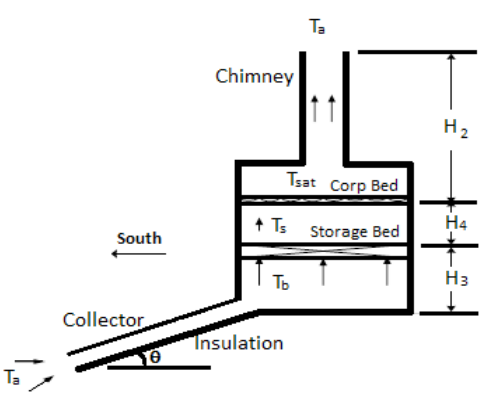

Figure (1). Indirect natural convective solar crop dryer with a storage bed below crop bed.

This design-type of solar dryers is similar to that considered by Sheriff [10] and Preston [11]. They

developed a mathematical model and presented results related to the behavior of the considered dryers to rice drying process. The objectives of the present work were to derive the appropriate equations under specific geometrical and operating assumptions [12]. This mathematical model was computed-based modeler that could be employed to predict the performance of the presently-studied indirect solar dryer. This work examined the effects of changing the location of the storage bed within the drying system. The effects of flow resistance, due to the amount of the storage bed thickness and the ratio of the void fraction, were considered.

3. MATHEMATICAL MODEL FOR THE SOLAR DRYER

The considered indirect solar dryer; Figure 1, may be divided into two parts; the flat plate solar collector and the drying chamber including pebble bed thermal storage and the crop bed. Hence, three control volumes were used in developing the mathematical models. Each was associated with a corresponding mathematical set of formulas.

Referring to the geometrical and operating conditions of the considered indirect solar dryer, there were several simplified-assumptions, including; the crop bed had a relatively small thickness, the rate of moisture removal depends solely on the moisture carrying capacity of the drying air, the amount of moisture removed was indicated by the air outlet temperature of the crop bed, and the moisture content would drop from its initial value until it became equal to the Equilibrium Moisture Content (EMC) corresponding to the conditions of the air entering the crop bed.

4. THE STORAGE BED

Taking a control volume around the pebble bed thermal storage, and applying continuity, momentum and energy basic equations, under the specified assumptions, leads to three different equations. There were several forces involved in the considered model, including; pressure, friction, body, and inertia forces. The buoyancy force is the most important force in the process. It is generated due to the presence of the differential pressure gradient along the height of the drying chamber. Generally, pressure drop across the storage bed depends mainly on the velocity, viscosity and density of the involved air, the bed void fraction, and the mean diameter of the pebbles. Since the pebbles diameter was being assumed small relative to the bed thickness, the simple Darcy model is used for evaluating the pressure drop that occurs across the storage bed [13]. This model gives the pressure drop as a function of air velocity in the drying chamber, the viscosity of the air, and the permeability of the rock bed, which can be obtained from the following equation;

$$\Delta P_s = \frac{U_d t_s}{K_s} \quad \text{..... (1)}$$

and

$$K_s = \frac{K}{\mu} \quad \text{..... (2)}$$

Where:

ΔP_s = pressure drop across storage bed.
U_d = mean velocity of air in drying chamber.
t_s = thickness of storage bed.
K_s = the storage bed pressure drop coefficient.
K = bed permeability.
μ = absolute viscosity.

According to previous studies, a value of $K_s = 7 \times 10^{-4}$ m²/Pa.s was taken [3,11]. The buoyancy force results from the pressure gradient which depends on the temperature gradient of the air in the dryer cabinet. Taking the order of magnitude, the pressure drops across the storage bed and across the crop bed were found to be the dominant pressure drops [3]. Here, the thickness of the crop bed was assumed to be small (a thickness of less than 40 mm). Hence, a linear relationship between the pressure drop across the bed and the velocity of air in the drying chamber has been assumed. Consequently, the crop bed pressure loss was treated in a manner similar to that across the storage bed. Referring to pressure-related Darcy model, the pressure drop across both beds together was expressed as follows:

$$\Delta P = U_d\left(\frac{t_r}{K_r} + \frac{t_s}{K_s}\right) \quad \text{..... (3)}$$

Where:

t_r = the thickness of the crop bed.

K_r = the crop bed pressure drop coefficient. The value of K_r was taken to be equal to 5×10^{-4} and 1.5×10^{-3} m^2/Pa.s, for rice and tomatoes, respectively [14,15]. The air was always assumed to leave the crop bed at saturated state condition [14].

The inertia force is small and could be neglected, due to light density of the flow and due to the low flow velocity. Using the Boussinesq approximation, the buoyancy force was assumed to balance the pressure drop across the crop and storage beds. This takes the following form [16]:

$$\beta g\rho\left[(T_b - T_a)\left(\frac{L(\sin\theta)}{2} + H_3\right) + (T_s - Ta).H_4\right] = U_d\left(\frac{t_r}{K_r} + \frac{t_d}{K_s}\right) \quad \text{..... (4)}$$

This equation represents the buoyancy force along the drying system, from the entrance of the collector at the bottom of the exit section of the drying chamber at the top. This force equals the pressure force across both beds. Other duct frictional forces are minor and thus omitted from the formula. Different new parameters are defined as follows:

β = bulk coefficient of expansion of air.
g = the acceleration of the earth gravity.
ρ = density of air.
L, H_3 and H_4 = dimensions of the drying system.
T_a = ambient air temperature.
T_b = temperature of air leaving collector.
T_s = temperature of air leaving storage bed.
θ = the collector tilt angle.

5. THE AIR COLLECTOR

This air collector was assumed to be simply constructed. It consists of a flat plate absorber with a glass-transparent top cover, where the hot air flows over the absorber and below the glass. The absorber was assumed to be well insulated from the back and sides of the collector. The collector has tilted to an angle of θ to the horizontal and it was facing south. The collector is wide with respect to its height, hence the air flow is considered to be two-dimensional flow [17].

Only the thermal energy losses from the cover of the collector, which were relatively the dominant, were considered. The bottom, sides of the collector, and the drying chamber were considered to be fully insulated. These losses depend on the temperature differential between the absorber-plate temperature and the ambient air temperature. Accordingly, the efficiency of the solar air-collector could be represented by:

$$\eta = A - \frac{B(T_p - T_a)}{q_i} \quad \text{..... (5)}$$

Where:

η = the efficiency of the collector.
q_i = the hourly solar radiation on collector surface, W/m^2.
T_p = the temperature of the absorber collector plate, K.
A and B are determined to be special constants.

The values of A and B represent the characteristics of the absorber plate and transparent cover [16]. Figure 2 compares the values used here with the range of experimental observed values for simple collectors with one cover plate [18].

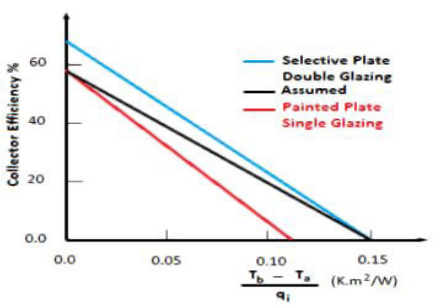

Figure (2). Assumed collector performance.

The instantaneous thermal efficiency of the solar air-collector, η, was given by:

$$\eta = \frac{q_c}{A_c q_i} \quad \text{..... (6)}$$

Where:

q_c = the useful thermal energy.
A_c = the area of the collector, m^2.

Referring to the energy equation, the useful sensible thermal energy was given by:

$$q_c = m_a C_p (T_b - T_a) \quad \text{..... (7)}$$

Where m_a = the mass flow rate of the air through the collector and could be calculated from the following relation:

$$m_a = \rho U_d A_d \quad \text{..... (8)}$$

Where: A_d =the cross-sectional area of the drying chamber. Equations (6, 7, and 8) are sufficient to determine the temperature of the air leaving the collector. Temperature difference could be given by the following:

$$(T_b - T_a) = \frac{\eta A_c q_i}{\rho U_d A_d C_p} \quad \text{..... (9)}$$

The rate of heat transfer between the absorber collector plate and the air passing through the collector is given by:

$$hA_c (T_b - T_a) = A_c \eta q_i \quad \text{..... (10)}$$

Where: h = the heat transfer coefficient between the absorber collector plate and the moving air. Equations (5) and (10) were combined to give the efficiency of the collector as:

$$\eta = \frac{Ah}{B + h} \quad \text{..... (11)}$$

Referring to the simulation of the natural convective heat-transfer rate, an appropriate well known relationship was adapted, where the heat transfer coefficient was arranged as follows [3]:

$$h = \left(\frac{Ck_a}{L}\right)\left(\frac{a_d}{a_c}\right)^{0.5} (Re)^{0.5} \quad \text{..... (12)}$$

Where:

a_c and a_d = the cross-sectional area of the collector and of the dryer chamber, respectively.

k_a = the thermal conductivity of the air.

C = a constant depends on the solar collector type.

Re = the Reynolds number based on the air velocity through the drying chamber and on the solar collector length.

Then, using Equations (4) and (9), Re-related relationship was arranged to have the following form:

$$(Re)^2 = \left(\frac{\beta g \rho^2}{\mu^2}\right)\left[\left(\frac{L^4}{k_a}\right)\left(\frac{\sin\theta}{2} + \frac{H_a}{L}\right)\left(\frac{w}{L}\right)\left(\frac{\eta q_i k_a}{C_p}\right) + \mu\, Re\, L(T_s - T_a)H_4\right] \times \left(\frac{K_r K_s}{K_s t_r + K_r t_s}\right) \quad \text{.... (13)}$$

Since the collector efficiency depends on the unknown h, which depends on the unknown induced air velocity, an iterative solution procedure should be followed. Starting with an assumed value for the collector efficiency, η, the estimated air flow rate was calculated. This allowed Re to be found and an improved η value could then be determined. The steps should be repeated until convergence was achieved.

The rate of change of storage bed temperature could be evaluated. For the exit air-temperature from the bed that was approximately equal to the bed temperature, the thermal energy balance for the storage bed could be represented as follows:

$$\rho U_d A_d C_p (T_b - T_s) = M_s C_s \frac{dT_s}{dt} \quad \text{..... (14)}$$

Where:

C_p = the specific heat of air at constant pressure.

M_s = the mass of the storage rock-material, kg.

C_s = the specific heat of the rock, J/kg.K.

This equation states that the rate of thermal energy gained by air flow across the storage bed is equal to the rate of thermal energy lost from the storage bed. In terms of enthalpy, Equation 14 became as follows:

$$m_a (h_b - h_s) = M_s C_s \frac{dT_s}{dt} \quad \text{..... (15)}$$

Where h_b and h_s are the enthalpy of the air entering and leaving the storage bed, J/kg, respectively. Referring to the thermal energy balances and rearranging, the saturation enthalpy, h_{sat}, of the air leaving the crop bed can be given by the following relation [3]:

$$h_{sat} = Ta + \frac{1}{(1 - \phi)}\left(\frac{\eta q_i A_c}{\rho U_d A_d} - C_p (T_b - T_s)\right) \quad \text{... (16)}$$

Where: ϕ = the relative humidity of the air and it is defined as the ratio of the mass of water vapor to the mass of water vapor required to produce a saturated mixture at the same temperature. The rate at which moisture is removed from the crop could then be found by applying the moisture mass balance for the crop bed as follows:

$$m_r \frac{dM_c}{dt} = m_a(\omega_{out} - \omega_a) \quad \text{..... (17)}$$

Where:

m_r = the mass of the dry crop bed, kg.

Mc = the moisture content of the crop.

m_a = the mass flow rate of the air flow.

ω_a = the moisture content of air at ambient conditions.

ω_{out} = the moisture content of air at the exit from the crop bed [3].

This equation is used to calculate the change in moisture content of the crop time. The calculation process should be stopped when the moisture content drops close to the Equilibrium Moisture Content, and reaches a value that is equal or below the required moisture content for long-term crop-storage.

A computer-based model for the natural convective indirect solar crop dryer associated with a storage bed was developed. Beside the dimensions of the dryer, this program requires a number of input data. Table 1 presents different input parameters [14,15]. Figure 3 shows a typical variation of the average-daily solar insolation; q_i, at 32°N location in September [19].

Table 1 Additional input parameters.

Parameter	Symbol	Value
Crop bed thickness	t	40 mm
Storage bed thickness	t_s	50 mm
Density of the rocks	ρ_s	2500 kg/m^3
Specific heat of the rocks	c_s	0.88 kJ/kg.K
Ambient air temperature	T_a	30°C
Ambient relative humidity	ϕ	50%
Initial crop moisture content (rice)	M_i	32 %
Initial crop moisture content (tomato)	M_i	94 %
Viscosity of the air	μ	1.9×10^{-5} N.s/m^2
Conductivity of the air	k_a	0.026 W/m.K
Initial collector efficiency	η	0.1
Crop density	ρ_r	600 kg/m^3
Pressure loss factor for crop (rice and tomato)	K_r	5×10^{-4} and 1.5×10^{-3} m^2/Pa.s
Pressure loss factor for storage	K_s	7×10^{-4} m^2/Pa.s
	A	0.56
	B	4.31 W/m^2.K
	C	1.1

The dryer was operated under no-load conditions, continuously for two days with about ten heating hours during each day in order to prepare the system with raising the temperature of the storage bed. Due to the closure of drying system during the night, the storage bed temperature at the beginning of the second day was assumed to be equal to that temperature at the end of the first day.

As a special treatment, according to 24-hours working day, during night hours, there was no incident solar insolation, and the temperature of the absorber plate decayed to be equal to the ambient temperature. This led to having another version of the above governing equations. Hence, the above equations became as follows:

$$\Delta P = U_d\left(\frac{t_r}{K_r}\right) \quad \text{..... (18)}$$

$$U_d = \beta g \rho [(T_s - T_a)H_4]\left(\frac{K_r}{t_r}\right) \quad \text{..... (19)}$$

$$Re = \frac{\beta g \rho^2 L}{\mu}[(T_s - T_a)H_4]\left(\frac{K_r}{t_r}\right) \quad \text{..... (20)}$$

$$T_{si+1} = \frac{1}{\beta\left(\frac{\rho U_d C_p}{\rho_s t_s C_s}\Delta t\right)}\left(\left(e^{\left(\frac{\rho U_d C_p}{\rho_s t_s C_s}\Delta t\right)} - 1\right)T_a + T_{si}\right) \quad \text{..... (21)}$$

$$h_{sat} = T_a - \frac{1}{(1-\phi)}(C_p(T_a - T_s)) \quad \text{..... (22)}$$

Where different parameters were defined as above. Here, T_s is the temperature of the air leaving storage bed, where it decreases throughout the night due to the continuous drying process. More details regarding the mathematical model, geometrical and operating scenarios are presented elsewhere [12].

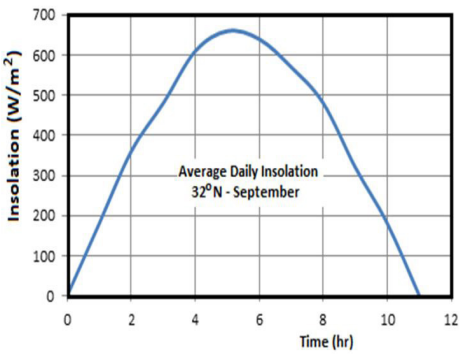

Figure (3). Variation of the average-daily solar insolation throughout the day.

6. RESULTS AND DISCUSSION

Referring to the mathematical model described above, a "QBASIC" computer program was written and applied in order to predict the variation of the moisture content of both rice and tomato with time. This necessitated the knowledge of several basic parameters which include; determination of the site location leading to the behavior of the solar insolation and mean ambient air conditions during the average-monthly day, configuration of the drying system, solar air collector and dryer dimensions, thermal and optical collector characteristics, tilt angle, bed thicknesses, initial and final required moisture contents, and pressure loss factors for different parts of the system.

The dimensions of the solar air collector are 0.7 × 0.7 m with a gap of 40 mm between the collector absorber plate and the glass cover. The dryer chamber is about 0.9 × 0.9 m^2 in cross section. This is similar to that system described by Bassey [20]. Table 1 presents various additional input parameters.

The initial storage bed temperature was assumed to be ambient temperature and the values of the solar insolation throughout the average-monthly day had been assumed to be fixed for the required days to complete the drying process. Using these input data, the dryer was first assumed to be operated under no-load conditions for two preparation days. Then the crop was placed in the dryer and the drying process started. The program was activated and the variation of moisture content with time was calculated.

There are two operational and calculating modes; one considers the variations that can take place only at working day hours while at night the system is closed. The other mode considers 24 working hours, including night hours at which the system should be evaluated [3,10,11,13]. The 24 hour scenario was adapted in the present study.

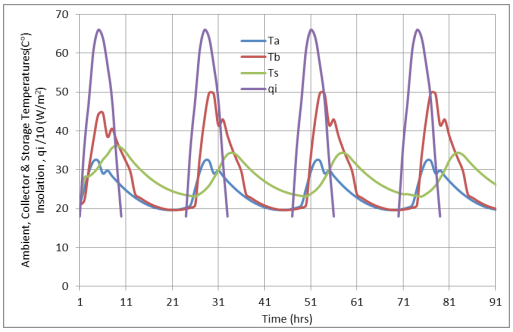

Figure (4). Variation of insolation, ambient, collector exit and storage bed temperatures with time for tomatoes dryer operating during 24 hours.

With respect to the storage pebble bed at a location below tomatoes bed, under the same above

geometrical and climatic conditions. Figure 4 shows the variation of the solar insolation, ambient, collector's exit, and storage bed temperatures during several 24-hour-mode working days. The effect of the overnight operation on the storage bed temperature history should be clear, where it takes almost sine-wave shape with a delay-shift of about four hours compared to the collector exit temperature distribution. The variation of the temperature at the exit of the air solar collector reaches a sort of steady shape by the second day of operation, with almost the same shape of temperature profile.

Figure 5 presents the variation of the collector exit and storage bed temperatures during the solar-drying days, for storage located below rice bed, for the 10-hour-mode operational solar day. Here, the air temperature leaving the solar collector has almost the same trend as that of the solar insolation, presented in Figure 3, with shifted-higher values from one day to the next.

The results show that the most important factors that affect the performance of the existing indirect-solar dryer are the height of the storage bed above the collector outlet; H_3, and the height of the crop bed above the storage bed; H_4. Figures 6 and 7 present the effect of such heights on the performance of the considered dryer. Figure 6 shows the variation of the moisture content of rice with solar time for different storage bed height; H_3, and for fixed height of the crop bed above the storage bed; H_4 = 1.0 m.

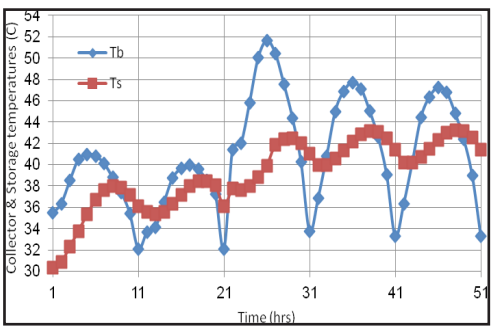

Figure (5). Variation of storage bed and collector exit temperature with time for rice dryer operating 10 hours per day.

As can be seen, there are significant improvements in dryer performance with increasing; H_3. Theoretically, this occurs as the buoyancy force below the storage bed is proportional to the height of the bed, where the higher the bed, the higher the buoyancy force. This leads to a higher flow rate through the dryer, and a higher rate of drying process. Logically, this could be looked as giving a chance for buoyancy and hence the induced flow momentum to be successfully generated as the distance increased before coming into the resistance associated with the storage bed. However, this may be limited to a certain range above which there is no sensed improvement.

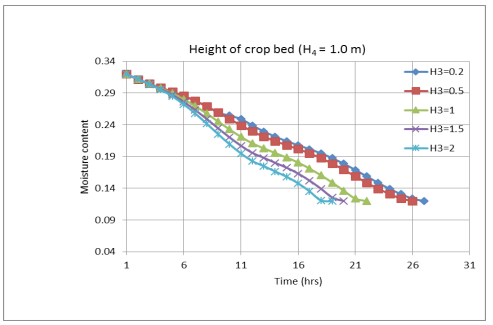

Figure (6). Effect of storage bed height, H3, on rice bed drying performance.

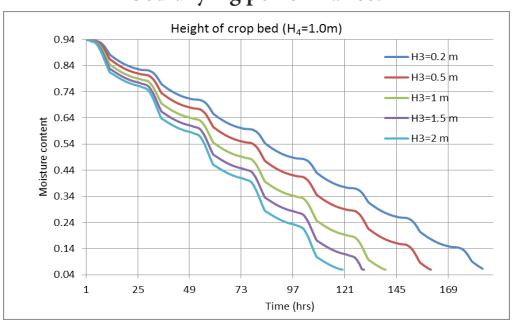

Figure (7). Effect of storage bed height, H3, on tomatoes bed drying performance.

Figure 7 is identical to Figure 6 under the same conditions, except for tomatoes instead of rice. Here, due to the amount of the moisture content of both products, a longer time is needed for drying tomatoes. Another difference factor is the unequal final required moisture content, which is higher in rice compared to tomatoes. One could notice the

inclined wavy trend of the behavior, part of which is due to the continuous operation even at nights, where no solar insolation is received.

Figures 8 and 9 show the effect of the height of the crop bed above the storage bed; $H_{4,}$ for storage bed location of H_3= 0.5 m, for rice and tomatoes, respectively. A significant improvement is expected in dryer performance with increasing the height between the two beds. The required drying time could be reduced about ten hours when the considered height goes from 0.5 to 2.0 m. This can be interpreted as a result of the recovery needed for the induced flow after passing the storage bed and this could be seen as an enhancing tool for the flow motion.

The pressure drop across the storage bed was found to have a considerable effect on the drying rate. The bed pressure loss factor, K_s, mainly depends on the porosity, shape and configuration of the rocks used in the bed. Here, different values for K_s were considered to account for such variations related to pebble's geometry and layout characteristics. Figure 10 shows the effect of the pressure drop across the storage bed on the drying performance. Obviously, reducing pressure drop would enhance the drying performance. Referring to the conditions associated with the results presented in Figure 8, saving of two working days can be achieved in drying a batch of rice. These results have encouraging operational conditions that should be carefully considered.

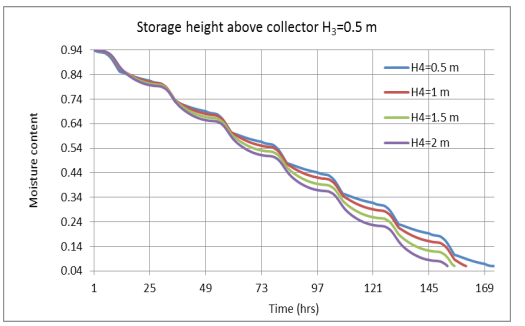

Figure (8). Effect of rice bed height, H4, on drying performance.

The pressure drop across the crop bed is expected to have the same effect. For any given flow rate, there will be a considerable pressure loss, which depends on grain-related factors including shape and size of the grain, configuration of the voids, and the bed thickness. Referring to the solar drying process related to previous published research work, the present results have the same trends while they are miss match in values. There is no base for comparison purposes due to different design, local air properties, sample moisture ratio, methodological conditions.

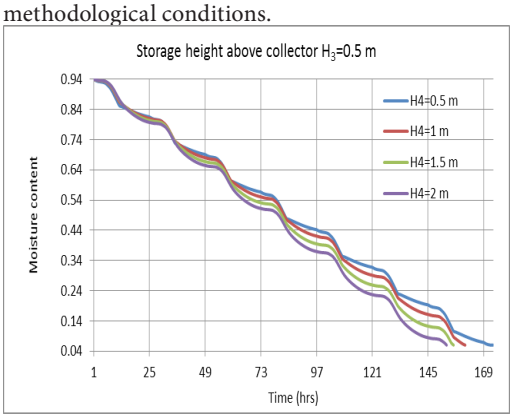

Figure (9). Effect of tomatoes bed height, H4, on drying performance.

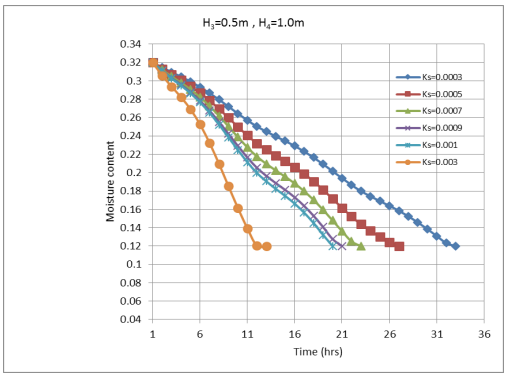

Figure (10). Effect of storage bed pressure drop factor n rice drying performance.

7. CONCLUSIONS AND RECOMMENDATIONS

According to the presented mathematical model and the corresponding various results, there are

general conclusions and recommendations could be stated in the following points:

1. The design details of the indirect solar dryer systems, including dimensions of system-components, position of the storage and crop beds, have direct effect on the performance of such dryers.

2. The characteristics of the storage and crop beds, such porosity, shape and size of bed units, and applied bed layout, influence the pressure drop across the beds, hence affecting the air flow, leading to dependable performance of considered dryers.

3. The most important property of the crop is the amount of the moisture content. This is clear when rice and tomatoes were compared. For rice, the drying process with such solar dryers is visible, while for tomatoes it takes several days to accomplish desired drying condition. Hence, it seems for crop products with high moisture content, such dryers are not applicable in agricultural fields that need relatively fast mass production in order to preserve the food within known time limit.

4. This study could be extended to cover the effects of storage and crop bed thicknesses, where optimizing study could be taken place in order to obtain an optimum set of design and operating conditions.

8. NOMENCLATURE

A	Constant in collector equation
A_c	Collector area – m^2
A_d	Area of drying chamber – m^2
a_c	Collector flow area - m^2
a_d	Drying chamber flow area - m^2
B	Constant in collector equation - W/m. K
C	Constant, dependent on the collector type
c_s	Specific heat of the rock - J/kg. K
c_p	Specific heat of air at constant pressure - J/kg. k
EMC	Equilibrium moisture content
g	Gravitational acceleration - m/s^2
H_2	Chimney height - m
H_3	height of storage bed above collector outlet - m
H_4	Height of crop bed above storage bed - m
H	Collector gap size - m
h	Heat transfer coefficient between collector plate and air - $W/m^2.K$
h_a	Enthalpy of ambient air - J/kg
h_s	Enthalpy of air leaving storage bed - J/kg
h_{sat}	Saturation enthalpy of the air - J/kg
K	Permeability - m^2
k_a	Thermal conductivity of the air - W/m.K
K_s	Storage bed pressure drop coefficient - $m^3.s/kg$
K_r	Crop bed pressure drop coefficient - $m^3.s/kg$
L	Dimension collector length - m
M_s	Mass of storage material - kg
m_a	Mass of air - kg
m_r	Mass of dry crop in bed - kg
m_{sat}	Mass of water in air at saturation - kg
m_v	Mass of water vapor in air - kg
Nu_L	hL/k_a
P_a	Water vapor pressure in the air- Pa
P_g	Saturation vapor pressure - Pa
P_v	Pressure of vapor - Pa
qi	Hourly solar radiation on collector surface - W/m^2
Re	Reynolds number based on u_d and length of the collector
Re_L	Reynolds number based on u_m and length of collector
T_a	Ambient air temperature - K
T_b	Temperature of air leaving collector - K

T_p	Temperature of collector plate - K
T_s	Temperature of air leaving storage bed - K
T_{sat}	Saturation air temperature - K
t	Time - s
t_r	Thickness of crop bed - m
t_s	Thickness of storage bed - m
U_c	Mean air velocity in collector - m/s
U_d	Mean air velocity in drying chamber - m/s
β	Bulk coefficient of expansion of air – K^{-1}
μ	Absolute viscosity - Pa.s
ρ	Density of air - kg/m^3
ρ_g	Density of saturated vapor - kg/m^3
ρ_r	Density of crop - kg/m^3
ρ_s	Density of rocks - kg/m^3
ρ_v	Density of vapor - kg/m^3
ϕ	Relative humidity
ω	Humidity ratio
ω_a	Moisture content of air at ambient conditions
ω_{out}	Moisture content of air at exit from crop bed
ω_{sat}	Saturation humidity of the air
η	Collector efficiency

9. REFERENCES

[1]. Liberty, J. T., Okonkwo, W. I., and Ngabea, S. A., Solar Crop Drying-A Viable Tool For Agricultural Sustainability And Food Security, International Journal Of Modern Engineering Research, Vol. 4. Iss. 6, June 2014.

[2]. Balakrishnan, A. R. and Pei, D. C. T., Heat Transfer in Fixed Beds, Ind. Eng. chem., Process Design and Develop., 13, 441-446, 1974.

[3]. Oosthuizen, P. H., Modelling of an Indirect Natural Convective Solar Rice Dryer, Proceeding of the Ninth Symposium on Engineering Applications of Mechanics, 434-441, May, 1988.

[4]. Schubert, R. C., and Ryan, L. D., Fundamentals of Solar Heating, Prentice-Hall, Inc., New Jersey, 1981.

[5]. Khama, R., Aissani, F., and Alkama, R., Design And Performance Testing Of An Industrial-Scale Indirect Solar Dryer, Journal of Engineering Science and Technology, Vol. 11, No. 9, 1263 – 1281, 2016.

[6]. El-Sebaii, A. and Shalaby, S.M., Solar Drying Of Agricultural Products: A Review. Renewable And Sustainable Energy Reviews 16.37-43, 2012.

[7]. Gross, R. J., Hickox, C. E. and Hackett, C. E., Numerical Simulation of Dual Media Thermal Energy Storage Systems, Journal of Solar Energy Engineering, ASME Trans, 102, 287-293 (1980).

[8]. Oosthuizen, P. H., Design of Natural Convective Solar Crop Dryers for Use in West Africa, Proceeding of the 15th Solar Energy Society of Canada, Penticton, B. C., 1989.

[9]. Sansaniwal, S. K. and Kumar, M., Analysis of ginger drying inside a natural convection indirect solar dryer: An experimental study. Journal of Mechanical Engineering and Sciences; Volume 9, pp. 1671-1685, December 2015.

[10]. Sheriff, A. Y., An Experimental Study of A Simulated Natural Convection Solar Rice Dryer, M.Sc. thesis, Queen's University at Kingston, 1987.

[11]. Preston, E. G. A., Simulation of A Natural Convection Solar Rice Dryer, M.Sc. thesis, Queen's University at Kingston, 1985.

[12]. Elbenghazi, E. M., Modeling The Thermal Behavior Of Indirect Solar Dryers Augmented with Pebble-Bed Thermal Storage, M. Sc. Thesis, University of Tripoli, Tripoli, Libya, 2013.

[13]. Bejan, A., Convection Heat Transfer, John Wiley & Sons, New York, 1984.

[14]. Excell, R. H. B., Basic Design Theory for A Simple Solar Rice Dryer, Renewable Energy Review Journal, 1, 2, 1, 1980.

[15]. Chavda, T. V., Agravat, S. M. and Philip, S. K., Drying of Tomato Using A Solar Dryer Incorporated with A LPG Back up, ISAE, 42nd Annual convection held at

CIAE, Bhopal, 474 – 496, 2008.

[16]. Duffie, J. A., and Beckman, W. A., Solar Engineering of Thermal Processes, John Wiley & Sons, New York, 1980.

[17]. Oosthuizen, P. H., A Numerical Study of The Performance of Natural Convection Solar Rice Dryers, Proceedings of the 5th International Symposium on Drying, Drying '86, Vol. 2, 670 -677, Boston, Massachusetts, August 13 - 15, 1986.

[18]. Sayigh, A. A. M., The Technology of Flat Plate Collectors in Solar Energy Conversion-An Introductory Course, eds. A. E. Dixon and J. D. Leslie, 101-124, Pergamon Press, Toronto, 1969.

[19]. Local Solar Insolation Data Report, Mean Monthly Solar Radiation Measurements, Information Department, Center For Solar Energy Studies, Tripoli, Libya, 1985.

[20]. Bassey, M. W., Influence of Chimney Configuration on Temperatures in A Solar Crop Dryer, Proceedings of Energex '82 Conference, Vo1.11/11, P. 862, August 23-29, University of Regina, Regina, Saskatchewan, Canada, 1982.